Atmospheric Environment 186 (2018) 18–31

Contents lists available at ScienceDirect

Atmospheric Environment

journal homepage: www.elsevier.com/locate/atmosenv

Dispersion simulations using HYSPLIT for the Sagebrush Tracer Experiment

Fong Ngan[a,b,*], Ariel Stein[a], Dennis Finn[c], Richard Eckman[c]

[a] Air Resources Laboratory, National Oceanic Atmospheric Administration, College Park, MD, United States
[b] Cooperative Institute for Climate and Satellites, University of Maryland, College Park, MD, United States
[c] Air Resources Laboratory, Field Research Division, National Oceanic Atmospheric Administration, Idaho Falls, ID, United States

ARTICLE INFO

Keywords:
WRF
HYSPLIT
Dispersion
Sagebrush experiment
Tracer

ABSTRACT

The Sagebrush experiment, led by NOAA's Field Research Division of the Air Resources Laboratory, consisted of five releases (intensive observation periods, or IOPs) of a chemically inert trace gas on five days in October 2013. All releases occurred in the afternoon under either near neutral stability conditions with high wind speeds or unstable conditions with low wind speeds. The sampling network for the tracer concentrations covered distances 200 m–3200 m from the release location and samples were obtained in 10-min averages. HYSPLIT, NOAA's transport and dispersion model, was used to simulate the spatial and temporal distribution of the tracer. The dispersion simulations were driven by WRF meteorological data with 27-km to 333-m grid spacing and using the inline and offline approaches as well as different planetary boundary layer schemes and a large-eddy simulation parameterization. Comparisons with measured wind speeds showed that none of the WRF PBL schemes or the large-eddy simulation parameterization was able to reproduce the rapid increase in high wind speeds observed during IOP3. The dispersion results were compared with the tracer measurements obtained during the experiment. The HYSPLIT dispersion simulations for IOP3, driven by the WRF data generated with various PBL schemes, showed greater concentration variability than the simulations performed for IOP5. The comparison between the inline and offline HYSPLIT simulations showed that the inline approach statistically outperformed the offline approach in three out of four IOPs because the tight coupling between the advection and dispersion processes implemented in the inline approach produced higher simulated concentrations close to the release location.

1. Introduction

Atmospheric transport and dispersion models are an important tool to understand, analyze, and forecast the movement of air masses and hazardous material in the atmosphere. HYSPLIT (Stein et al., 2015), NOAA's dispersion model, is one of the most commonly used atmospheric transport and dispersion models, and it has been adopted in routine operations to forecast wildfire smoke, wind-blown dust events, and a variety of chemical releases. This model has also been widely applied to study the source-receptor relationship of air pollutants (Cohen et al. 2013; Stein et al. 2007), nuclear incidents (Simsek et al., 2014; Chai et al., 2015), and volcanic ash events (Crawford et al., 2016; Chai et al., 2017). HYSPLIT relies on data from meteorological models, such as the Advanced Research dynamic core of the Weather Research Forecasting (WRF) model (Skamarock et al., 2008), to provide the required variables for the transport and dispersion calculation.

Given increasing interest in local-scale emission events and the availability of computational resources, both WRF and HYSPLIT have recently been configured and applied at high spatial and temporal resolutions (few hundreds of meters and minutes) to resolve local flow features (e.g. Sun et al., 2017; Powers et al., 2017; Rolph et al., 2017). However, the extent to which the models perform at fine scales and the most appropriate modeling configuration for high resolution scenarios remain unclear (Barlow et al., 2017; Powers et al., 2017; Shin and Dudhia, 2016). The Sagebrush tracer experiment (Finn et al. 2015, 2016), featuring inert chemical measurements taken within a 3-km range of the release location at 10-min temporal averages, offers a unique opportunity to test the simulation tools at high resolutions. The experiment provides a comprehensive set of surface and tower meteorological observations including wind and temperature soundings and profiles as well as fluxes to help understand the stability and mixing conditions along with tracer concentrations to study the transport and dispersion. One of the main goals of the experiment is to provide a high quality data set for testing and evaluating existing dispersion models. This study is the first attempt to analyze the Sagebrush experiment by using WRF to simulate the meteorology and HYSPLIT to model the dispersion. The sub-kilometer scales on which the Sagebrush experiment relies are comparable to the scales of large eddies whose

* Corresponding author. 5830 University Research Court, NCWCP, Rm 4207, College Park, MD, 20740, United States.
E-mail address: Fantine.Ngan@noaa.gov (F. Ngan).

https://doi.org/10.1016/j.atmosenv.2018.05.012
Received 5 March 2018; Received in revised form 7 May 2018; Accepted 8 May 2018
Available online 09 May 2018

characteristics are not satisfactorily captured by existing planetary boundary layer (PBL) parameterizations or large-eddy simulations (LES)(Shin and Dudhia, 2016).

Because HYSPLIT was originally designed to work offline from the meteorology, the parameters needed for the dispersion calculation are extracted and re-diagnosed after running a meteorological model such as WRF. Ngan et al. (2015) developed an inline approach by coupling HYSPLIT with WRF in such a way that the dispersion computation is embedded in the meteorological model without the need for post-processing, resulting in a more consistent depiction of the state of the atmosphere and dispersion simulation. Ngan et al. (2015) applied the inline HYSPLIT to two controlled tracer experiments featuring synoptic transport and nocturnal drainage flow conditions. The results of that work showed that the inline approach does not provide any sizable advantage over the offline approach for regional scale transport scenarios; however, it improves the simulation of fine spatial and temporal scales. Consequently, we expect Sagebrush to offer a good platform on which to evaluate the inline approach given the spatial and temporal characteristics of the tracer experiment.

This study aims to understand the transport and mixing processes that affect tracer dispersion in daytime convective conditions. In particular, by evaluating the meteorological and dispersion results with measurements taken during the Sagebrush tracer experiment, we assess the model's performance at a fine spatial and temporal scale. The structure of the remainder of this paper is as follows. Section 2 reviews the Sagebrush experiment and synoptic meteorological conditions during tracer releases. Section 3 describes the model configurations for the meteorological and dispersion models as well as simulation design for the different sensitivity tests. In Section 4, we evaluate the WRF and HYSPLIT simulations and in Section 5, we discuss the meteorological and dispersion results. Finally, Section 6 presents the conclusions and future research directions.

2. Sagebrush tracer experiment

The Project Sagebrush phase 1 (Finn et al. 2015, 2016) tracer field experiment was conducted at the Idaho National Laboratory during October 2013. The experiment was designed to test measurement technologies not available during the dispersion studies conducted in the 1950s and 1960s and to improve our understanding of short-range dispersion by performing a continuous near-surface inert tracer release over a flat terrain. The experiment consisted of five SF_6 releases (Table 1), so called Intensive Observation Periods (IOPs), on five days,

Table 1
A brief summary of all the releases in the Sagebrush tracer experiment. Note: data points are number of tracer measurement pairing to model concentrations used for statistical evaluations.

	IOP 1	IOP 2	IOP 3	IOP 4	IOP 5
Date (Oct 2013)	2nd	5th	7th	11th	18th
Start Time (MST)	1400	1230	1230	1330	1230
End Time (MST)	1630	1500	1500	1600	1500
Emiss rate (g/s)	10.177	9.986	9.930	1.043	1.030
Emiss total (g)	89049	89509	89605	9064	9031
Data points	1343	1341	1388	1313	1363

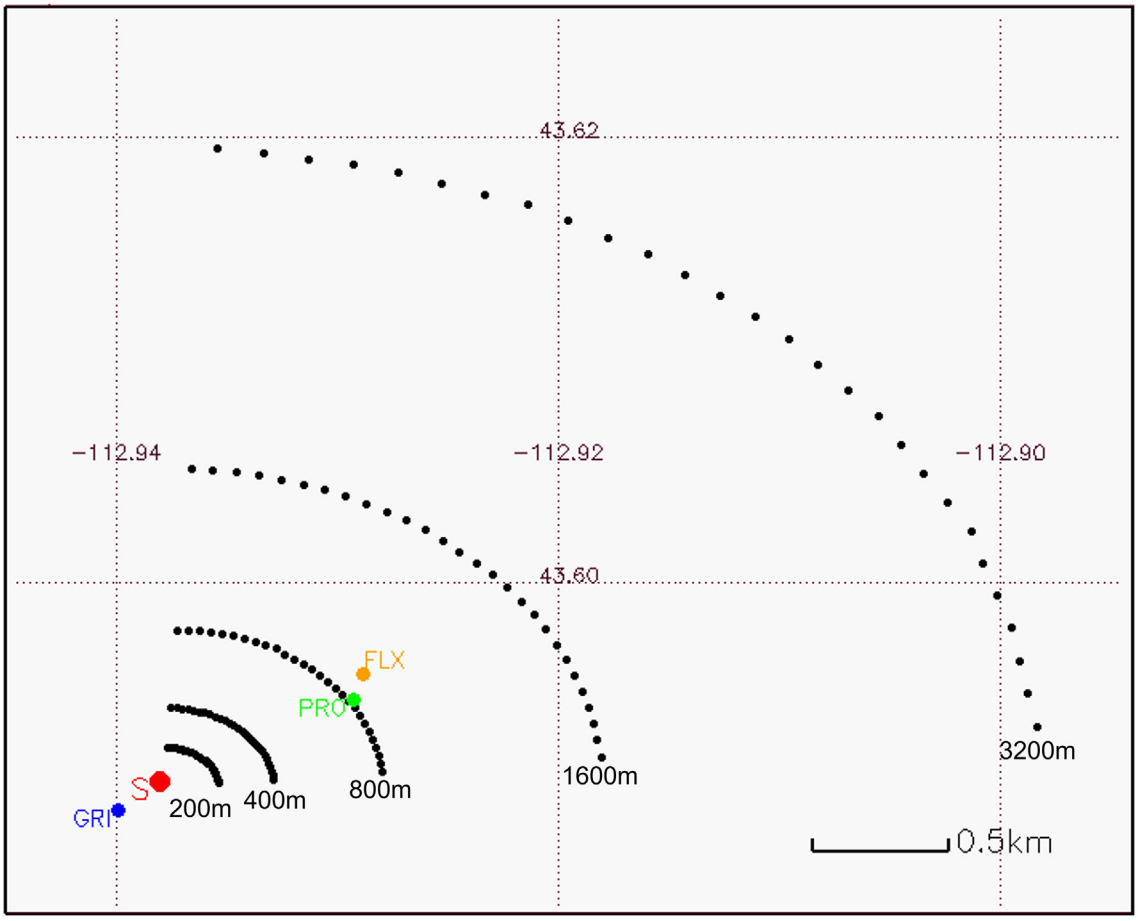

Fig. 1. Sampling network for tracer measurements (black dots) for the Sagebrush tracer experiment. The red dot (labeled “S”) is the release location of tracer. Meteorological measurements are the Grid 3 tall tower (blue dot, labeled “GRI”), the wind profiler (green dot, labeled “PRO”) and the station taking flux measurements (orange dot, labeled “FLX”). (For interpretation of the references to color in this figure legend, the reader is referred to the Web version of this article.)

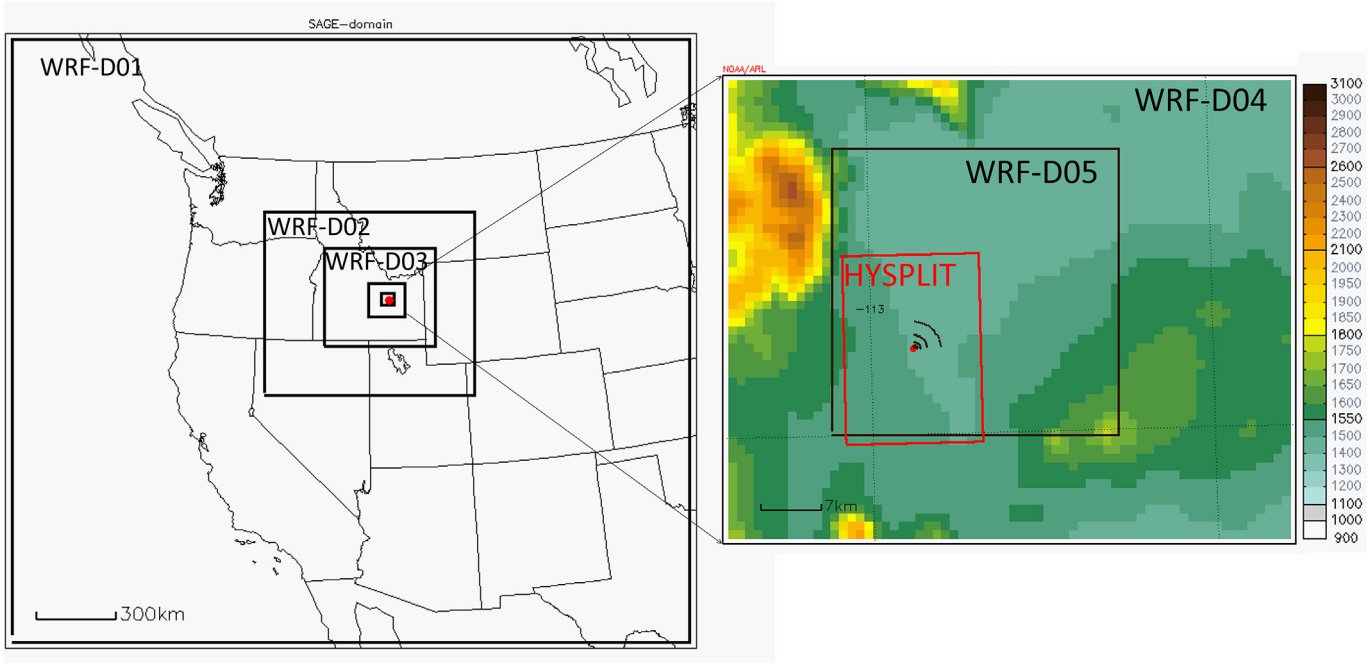

Fig. 2. Domain configuration for Sagebrush tracer experiment. Black-line boxes are the five nested domains for WRF simulations and the red-line box is the HYSPLIT domain. Black dots are tracer sampling networks and the red dot is tracer release location. The color background represents model terrain height. Unit: meter. (For interpretation of the references to color in this figure legend, the reader is referred to the Web version of this article.)

Table 2
Model configuration for WRF simulations.

	D01	D02	D03	D04	D05
Grid spacing	27 km	9 km	3 km	1 km	0.333 km
IC/BC	3-hourly NARR			D03 nestdown	
Nesting	2-way nesting			2-way nesting	
Microphysics scheme	WSM3[a]			WSM3	
Cloud scheme	Grell-Freitas ensemble scheme[b]			None	
Radiation scheme	RRTMG[c]			RRTMG	
PBL scheme	Various PBL schemes [h]			YSU or MYJ	
Surface scheme	Schemes corresponding to PBL schemes [h]			Monin-Obukhov similarity theory MM5[d] or Janjic[e]	
Land surface model	Noah LSM[fi]			Noah LSM	
Nudging	3D n0udging[g] (nudge PBL wind)		3D nudging (no PBL wind)	None	
Time step	90 s	30 s	10 s	3 s	1 s
Output frequency for offline HYSPLIT	1 h	1 h	5 min	5 min	5 min

[a] WRF single-moment three-class (Hong et al., 2004).
[b] Grell and Freitas (2013).
[c] Iacono et al. (2008).
[d] MM5 similarity theory (Grell et al., 1994).
[e] Janjic (1994).
[f] Noah land surface model (Chen and Dudhia, 2001).
[g] Analysis grid nudging (Deng et al., 2009).
[h] Refer to section 3a.
[i] Except AMC2 PBL scheme paired with the Pleim-Xiu LSM (Xiu and Pleim, 2001).

all occurring in the afternoon under either neutral stability conditions and high wind speeds or unstable conditions and low wind speeds. The tracer was released on relatively a flat terrain located at an elevation of about 1500 m above mean sea level surrounded, on the western side, by mountain chains over 3000 m and, on the eastern side, by a lower mountain range.

Fig. 1 shows the layout of the measurement array for the tracer concentrations. The sampling network consisted of concentric arcs located 200, 400, 800, 1600, and 3200 m away from the release location. The tracer was released at a constant rate over two-and-a-half hours and sampling started 30 min after the release, producing 10-min average measured concentrations. Comprehensive meteorological measurements were obtained during the days when the releases occurred including surface stations, radiosondes, wind profilers and towers with 3D sonic anemometers to fully characterize the state of the boundary layer. In this study, we used data collected at the Grid 3 tower (GRI) located southwest of the tracer release site, the wind profiler (PRO) located at the 800-m arc, and the energy flux station (FLX) taking measurements about 900 m NE of the release point (Fig. 1).

IOP1 was excluded from this study because the wind flow patterns caused the tracer plume to go in the opposite direction of the sampling array (i.e., the plume was not captured by the network; Finn et al., 2015). The day of IOP2 was mostly sunny with relatively light winds (under $^{3\,ms\text{-}1}$) in the early afternoon but slightly increasing (up to $^{4\,ms\text{-}1}$) later in the tracer period. The wind directions varied but were mostly southerly to southwesterly in the afternoon. This case showed more favorable conditions for advecting the tracer to the sampling network compared with IOP1. On the day of IOP3, nighttime temperatures reached freezing but increased to about 20 °C in the afternoon. Calm wind conditions prevailed during the morning. At about noon, when the release took place, a southwesterly wind developed and rapidly increased to $^{8\,ms\text{-}1}$ throughout the rest of the afternoon. For IOP4 and IOP5, the synoptic weather conditions were similar to those during IOP3 – mostly sunny with moderate southwesterly winds and weak unstable conditions. The flows were relatively stationary during the release periods providing good conditions for advecting the tracer across the sampling network.

3. Modeling designs

3.1. WRF model configuration

The WRF model (version 3.7) was configured with five domains (Fig. 2) with horizontal grid spacing of 27 km (D01), 9 km (D02), 3 km

Table 3
Mean Absolute Errors (MAEs) of surface wind speed, wind direction and temperature from WRF simulations with different PBL schemes using observations during 11–17 MST on the days of IOP3 and IOP5.

	IOP3			IOP5		
	Wind speed (ms^{-1})	Wind direction (degree)	Temperature (°C)	Wind speed (ms^{-1})	Wind direction (degree)	Temperature (°C)
YSU	3.792	19.125	1.575	0.868	25.387	0.868
MYJ	3.274	18.554	1.455	0.930	25.608	1.030
QNSE	4.348	56.327	1.806	1.281	25.965	1.002
MYNN	4.009	22.534	1.999	0.866	25.036	0.837
ACM2	3.704	25.779	1.071	0.881	22.402	2.002
BouLac	3.860	19.306	1.623	0.835	25.274	0.896
UW	3.494	19.124	1.544	0.829	25.761	0.909
TEMF	3.529	22.269	1.394	1.007	26.254	2.453
GBM	3.574	19.989	1.441	0.848	25.549	0.873

(D03), 1 km (D04) and 0.333 km (D05). We set 20 vertical layers within the PBL with the first mid-layer height of the model at around 8 m. The WRF simulations for the outer three domains were initialized by using the North American Regional Reanalysis (Mesinger et al., 2006) with 32-km grid spacing and available every 3 h. For the inner two domains, the WRF results from the coarser domains were nested down to provide the initial and boundary conditions. Table 2 summarizes the model configuration and physics options used in the simulations.

Among all the physics processes included in the WRF model, PBL characterization and its corresponding surface scheme are fundamental for dispersion applications. Each of the many options to parameterize PBL development behaves differently depending on the atmospheric conditions. Consequently, we performed sensitivity tests on the outer three domains for IOP3 and IOP5 to understand the most appropriate PBL parameterization for conditions such as those encountered during the Sagebrush experiment. These two IOPs were selected for the sensitivity tests because they represented two different stability conditions; neutral for IOP3 and weakly unstable for IOP5. Both were captured well by the sampling network throughout the release. Yet, IOP3 was a more difficult case due to the strong southwesterly wind, while IOP5 featured a gradual increase in the southwesterly wind in the afternoon. The PBL scheme test included the Yonsei University (YSU; Hong et al., 2006), Mellor-Yamada-Janjic (MYJ; Janjic, 1994), Quasi-Normal Scale Elimination (QNSE; Pergaud et al., 2009), MYNN 2.5 level TKE (MYNN; Nakanishi and Niino, 2006), ACM2 (ACM2; Pliem, 2007), Bougeault and Lacarrere (BouLac; Bougeault and Lacarrere, 1989), University of Washington (UW; Bretherton and Park, 2009), Total energy mass flux (TEMF; Angevine et al., 2010), and Grenier Bretherton MaCaa (GBM; Grenier and Bretherton, 2001) schemes. Note that the simulations were performed with the PBL schemes and their corresponding surface layer schemes, except for the YSU, BouLac, UW, and GBM cases in which the MM5 Monin-Obukhov surface scheme was applied. Table 2 lists the other physics options. The WRF results of IOP3 and IOP5 were evaluated with meteorological measurements taken during the experiment. Then, the WRF meteorological data generated based on the various PBL schemes were used to drive the HYSPLIT simulations and the dispersion results were evaluated against the measured concentrations. Based on the performance of the meteorological and dispersion simulations, we selected two mixing parameterizations (i.e., the YSU and MYJ PBL schemes) to run the WRF simulations at higher spatial resolutions, namely 1-km and 0.333-km horizontal grid spacing, for all the Sagebrush experiment IOPs. Additionally, we applied both the offline and the inline versions of HYSPLIT and compared the results with the tracer measurements.

3.2. HYSPLIT dispersion simulation

HYSPLIT was set to simulate a continuous tracer release lasting two-and-a-half hours from a source located at 43.59 °N and 112.94 °W, 10 m above ground level, using 250,000 Lagrangian particles. Table 1 lists the starting time and emission rate of each IOP. The concentration grid was set with a horizontal resolution of ~100 m with one vertical layer extending from 0 to 25 m above ground level. The model concentration output was averaged at a 10-min frequency to match the measurements. In addition to running the standard HYSPLIT (offline), we applied the inline coupling version of WRF-HYSPLIT to the Sagebrush experiment. The model configurations for both meteorology and dispersion were identical to that of the offline HYSPLIT. However, unlike the offline HYSPLIT, which used WRF data outputs every 5 min, the inline HYSPLIT was driven by meteorological data at the WRF integration time step, which depended on the horizontal grid spacing of the domain (Table 2).

4. Evaluation of the WRF and HYSPLIT simulations

4.1. WRF sensitivity tests for IOP3 and IOP5

One of the main contributors to the uncertainty in dispersion modeling is the meteorological data that determine the transport and mixing in the atmosphere. Before evaluating HYSPLIT, we assessed the WRF performance through quantitative (i.e. statistical calculation) and qualitative (i.e. visual comparison at stations) analyses against the observations available during the experiment. The WRF sensitivity simulations with various PBL schemes were conducted on the outer three domains (27-km, 9-km and 3-km grid spacing) for IOP3 and IOP5. For the statistical evaluation, we used a network of 20 mesonet sites spatially distributed within a 10–20 km radius of the tracer experiments measuring temperature and wind at 5-min intervals. Table 3 presents the mean absolute errors, (MAEs), for the surface temperature, the wind speed, and the wind direction. The meteorological evaluation aims to assess the quality of the WRF data later used to model the dispersion during the Sagebrush experiment. Thus, we computed the statistics using observations during 11–17 MST on the days of IOP3 and IOP5. WRF performed better for IOP5 than IOP3 as the mean absolute errors for surface temperature and wind speed were smaller in IOP5 than those in IOP3. Among the nine WRF runs using different PBL schemes, the QNSE showed the largest bias in wind speed prediction for both episodes.

For IOP3, the tower measurements showed stagnant conditions prevailing during the morning with rapidly increasing wind speeds, from about $^{2\,ms\text{-}1}$ to $^{8\,ms\text{-}1}$, in the afternoon (Fig. 3). The wind direction began to veer from easterly at around 11 MST and stayed southerly for the rest of the day. The WRF model under-predicted the rapid development of the strong south-southwesterly wind between 12 and 13 MST, the time when the SF_6 release started. As shown in the statistical summary, the QNSE scheme showed the worst performance among the nine PBL parameterizations, producing very low northeasterly winds throughout the day. The TEMF parameterization showed a sudden

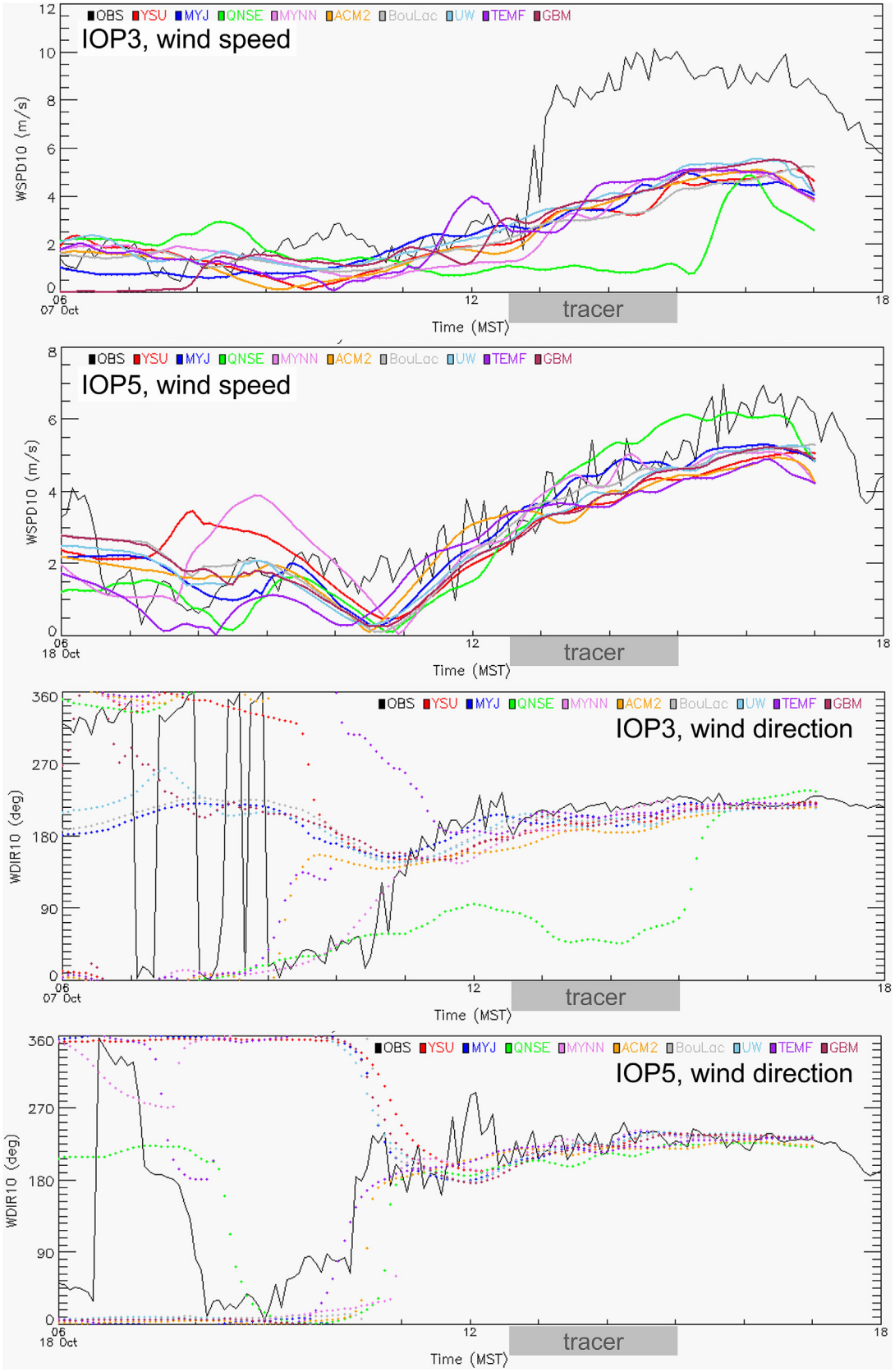

Fig. 3. Time series of observed and modeled 10-m wind speed (ms^{-1}) and wind direction (degree) at the GRI tower for IOP3 and IOP5 from 3-km WRF simulations using different PBL schemes.

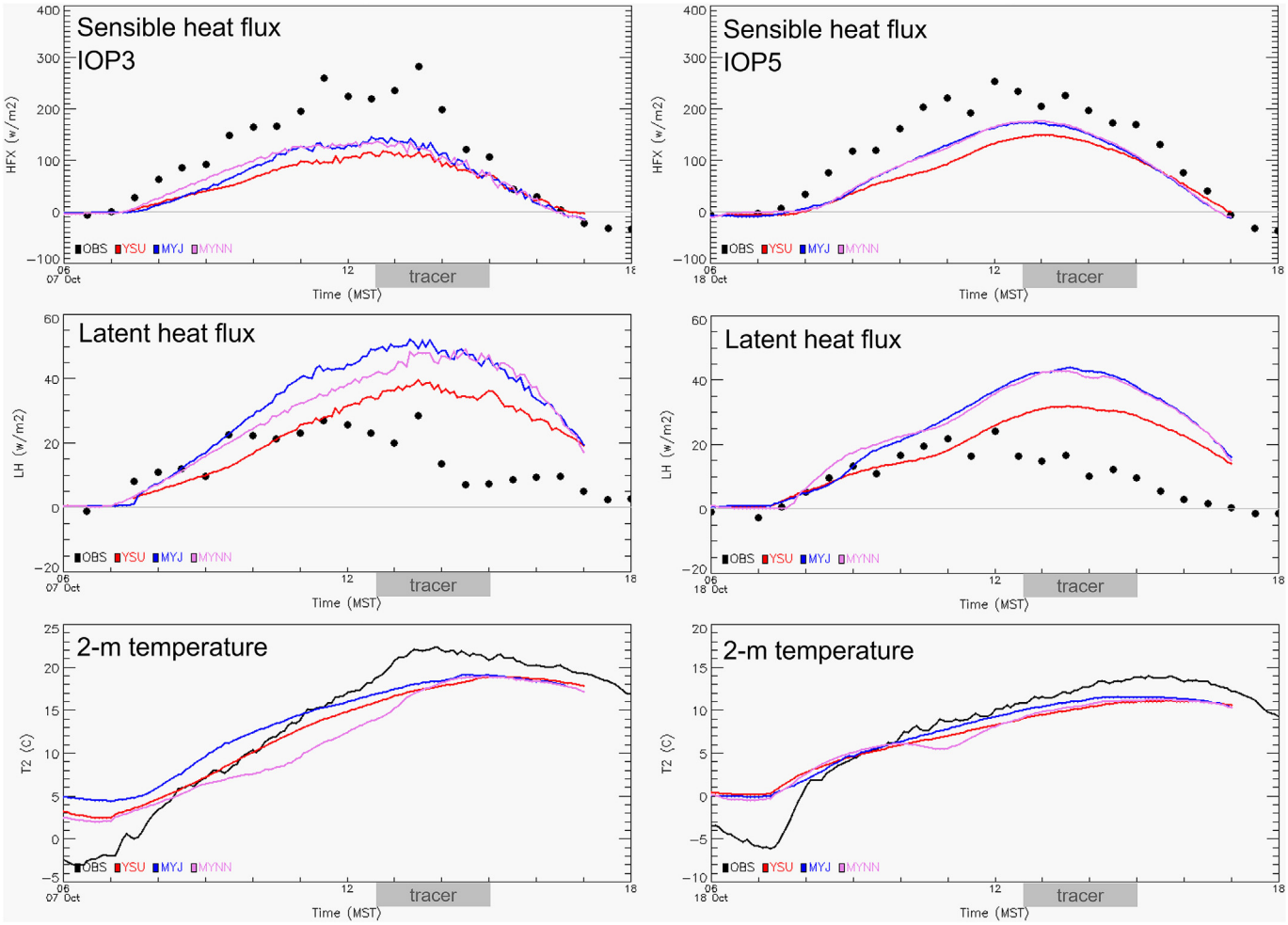

Fig. 4. Time series of observed and modeled sensible heat flux (wm^{-2}), latent heat flux (wm^{-2}) and 2-m temperature (°C) at the FLX stations for IOP3 (left) and IOP5 (right) from 3-km WRF simulations using different PBL schemes.

increase and decrease in wind speed resulting in a maximum around noon. The run corresponding to the MYNN scheme presented the slowest increase in wind speed compared with the other runs. On the contrary, for IOP5, the WRF model simulated well the gradual increase in wind speed in the late morning and its magnitude during the period of tracer release in the afternoon (Fig. 3). In addition, all the PBL schemes performed similarly in predicting the weather conditions for this episode, except for the QNSE run which showed generally higher bias in the afternoon.

Fig. 4 presents the heat fluxes measured at the FLX station along with the WRF results corresponding to the YSU, MYJ, and MYNN PBL schemes. The sensible heat flux was underestimated and latent heat flux was overestimated in the daytime. These biases imply that the WRF model does not partition the energy in the surface layer accurately, consistent with the findings of Gibbs et al. (2011) and Sun et al. (2017). The MYJ scheme and its corresponding surface physics scheme tended to simulate higher sensible heat and latent heat fluxes than the YSU scheme and its corresponding surface scheme. The comparisons of heat fluxes and thermal variables show that the WRF model performed similarly in simulating these fields for IOP3 and IOP5 regardless of the large difference in wind prediction in both episodes.

This experiment was conducted on a plain surrounded by a mountain range of about 3000 m to the north and northwest and a lower mountain range to the east. At night, over the experimental area, the surface temperature dropped due to radiative cooling and cool air advection from the mountains. In the morning, the surface was gradually heated by the solar radiation, producing a growth in the PBL height accompanied by an increase in wind speed at the surface. During the nighttime, the wind pattern from the surface up to 1 km, measured by the wind profiler (Fig. 5), was not simulated well by the model independent of the PBL scheme used. This can be attributed to inaccuracies in other components of the WRF model such as the surface layer scheme or land surface model. The surface temperature shows a warm bias during nighttime. When comparing the spatial temperature and the wind vectors plots obtained from the WRF simulations, the YSU parameterization predicted lower temperatures than MYJ in the area of the tracer release in the morning of IOP3 (Fig. 6). Further, the dissipation of the cold surface pool was modeled differently by the MYJ and YSU schemes, with the former showing a faster response than the latter. By noon, the MYJ parameterization produced a PBL a few hundred meters higher than that of the YSU (Fig. 5).

4.2. Dispersion results using different WRF data for IOP3 and IOP5

The 3-km WRF meteorological data generated with the various PBL schemes evaluated in the previous section were used to drive the HYSPLIT simulations and the results were compared with the measured concentrations. To evaluate the dispersion results, we used the rank, a cumulative score introduced by Draxler (2006). The rank includes four normalized components, namely – the correlation coefficient (R),

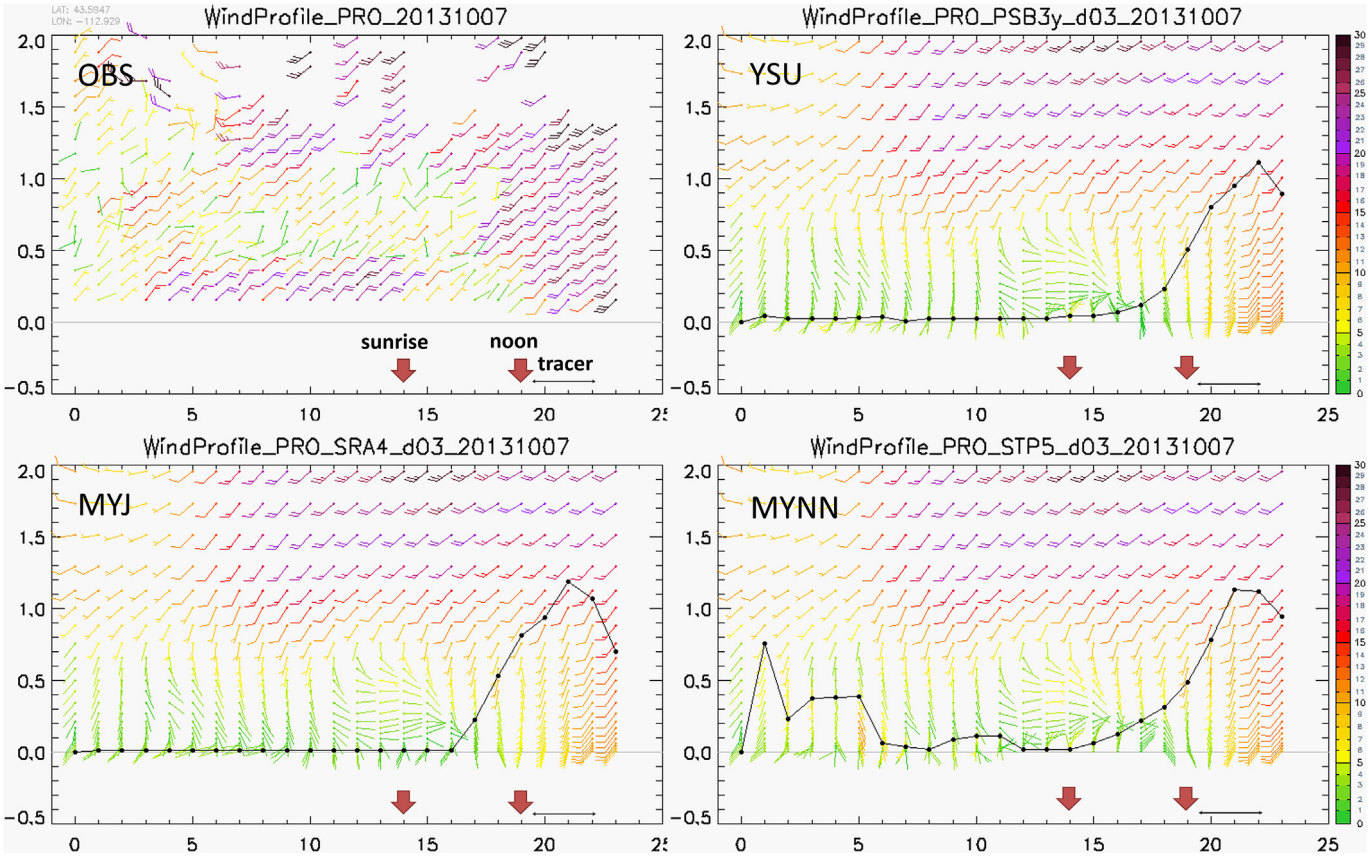

Fig. 5. Time series of wind profile plot on October 7th, 2013 (IOP 3). The x-axis is the hour in UTC and the y-axis represents the altitude (km). The black dotted line is the model PBL height at the site. Unit: knots.

fractional bias (FB), figure-of-merit in space (FMS), and Kolmogorov-Smirnov parameter (KSP), and it ranges from 0 (worst) to 4 (best). This statistical score has been used to evaluate the results of dispersion models in various studies (Stein et al., 2015; Hegarty et al., 2013; Eslinger et al., 2016; Leadbetter et al., 2015). Table 1 lists the number of measurement points paired with the HYSPLIT results for the evaluations.

Fig. 7 shows the statistical summary for the HYSPLIT results using the 3-km grid spacing WRF data. In general, the ranks for IOP3 were worse than those for IOP5 as WRF predicted the wind much better for IOP5 than IOP3. The dispersion results using the QNSE data show a poor rank that was consistent with the evaluation of the WRF results. Fig. 8 shows spatial plots of the modeled plume for the IOP3 case. Stagnant wind conditions generated by the QNSE parameterization in the case of IOP3 caused the plume to stay near the release location and even slowly move in the opposite direction of the measurement network. The dispersion pattern obtained based on the ACM2 meteorology was displaced about 10–15° to the north of the observed plume resulting in an almost zero R value and a lower FMS in the cumulative statistic score. The angle of the MYJ plume (as with the TEMF plume, not shown) entering the measurement network matched well with the observations but modeled concentrations at the farthest measurements stations are too high. The MYNN based dispersion simulation showed a wider plume more displaced to the north. The YSU plume, similar to the BouLac (not shown) and MYJ cases, shows a narrow pattern stretching out to the outermost arc; however, it was clearly misplaced too much to the north when compared with the observed plume which moved northeastward. For IOP5, all the simulations performed similarly except for the QNSE case as its associated plume was placed about 10 degrees off the observed plume.

4.3. Dispersion results for all IOPs

We conducted WRF simulations with the five-nested domain by using the MYJ and YSU PBL schemes for all four Sagebrush IOPs and performed HYSPLIT runs with these two meteorology sets. Although other WRF simulations based on different PBL schemes such as MYNN and TEMF generated dispersion results comparable to the simulations of MYJ and YSU, we selected the MYJ and YSU to represent two classes of PBL parameterizations, one based on the turbulent kinetic energy prediction and the other on a first-order diagnostic K-profile (Shin and Dudhia, 2016). Fig. 9 shows the statistical rank of the offline HYSPLIT results for different WRF domains and IOPs. The MYJ-based meteorology produced better dispersion results for IOP3 while the YSU-based meteorology generated a slightly better dispersion results for IOP5. Among the four releases, the model performed the best for IOP5, when the wind flow was constantly blowing from the northeast during the release period, providing good conditions to transport the tracer across the sampling network. On the other hand, Fig. 9 shows that the dispersion results for IOP 2, 4, and 5 were not sensitive to the grid resolution of the meteorological data.

When attempting to simulate increasingly higher spatial scales (of the order of a few hundreds of meters) we have to take into consideration that traditional turbulence modeling methods are not designed for spatial resolutions comparable with energy-containing turbulence scales (Shin and Hong, 2015) and we encounter the so-called “terra incognita” (Wyngaard, 2004; also called the gray zone) for subgrid-scale turbulence. On one hand, the use of the LES is recommended in the WRF model to resolve eddies for a domain with less than a 100-m grid size (Dudhia and Wang, 2014). On the other hand, a PBL parameterization should be used for horizontal grid spacing of 500 m or

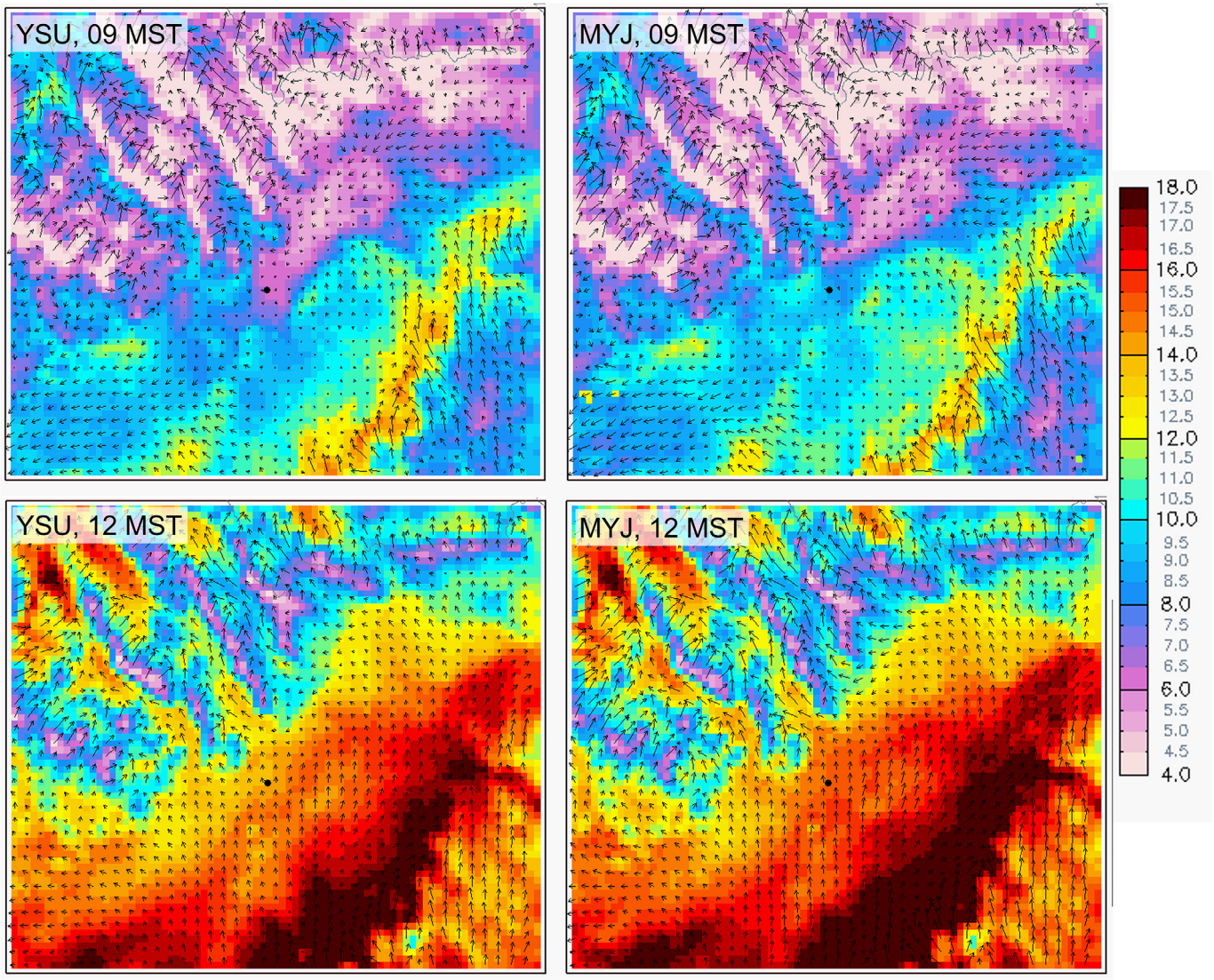

Fig. 6. Horizontal distribution of 3-km WRF simulations (YSU on the left panel and MYJ on the right panel) at two time steps during IOP 3 (09 MST and 12 MST October 7th, 2016). The shaded color represents surface temperature () while arrows indicate wind vectors. The black dot is the release location. (For interpretation of the references to color in this figure legend, the reader is referred to the Web version of this article.)

larger because eddies are unresolved at that scale. Therefore, for a grid size of 100–500 m, as in the finest domain in the Sagebrush tracer experiment, a PBL parameterization and the LES should be taken into consideration.

We ran two additional sets of simulations driven by the WRF data using the Shin-Hong PBL scheme (labeled SH) and the LES scheme for IOP3 and IOP5 at a sub-kilometer scale. Note that the Shin-Hong PBL scheme was designed to solve the subgrid-scale turbulent transport in convective boundary layers (Shin and Hong, 2015). The comparison of the wind speeds for the WRF simulations corresponding to the YSU PBL scheme, Shin-Hong PBL scheme, and LES showed that all three configurations generated similar surface winds during the daytime. The LES run featured a larger variation in the wind speed during IOP3 and an overprediction of the wind speed during IOP5 at nighttime. The HYSPLIT results driven by the simulations using SH and LES WRF data were not as good as the run using the YSU-based data. The LES run showed the worse rank due to a low correlation coefficient and a poor FMS compared with the results driven by the YSU and SH meteorology (Fig. 9).

5. Inline HYSPLIT simulations for the Sagebrush experiment

The inline version of HYSPLIT was applied to the Sagebrush experiment and the results were compared with the offline results through the evaluation with the concentration measurements. We ran both the inline and the offline HYSPLIT with the WRF domains using a 1- and a 0.333-km grid spacing for all four IOPs. The inline framework has the advantages over the offline approach of using higher temporal frequency of the meteorological data, as well as the same vertical coordinate system as WRF (no interpolation needed) for the dispersion calculation. Fig. 10 shows the statistical summary of the inline and offline HYSPLIT simulations driven by the WRF data based on the MYJ and YSU PBL schemes. For three out of four releases (all except IOP2), the inline results outperformed the offline simulations. Overall, the inline plumes had a better FMS and KSP than the offline plumes while the difference in rank between inline and offline was larger in the simulations driven by the MYJ-based data than the YSU-based data.

The spatial plots (Figs. 11–13) show that the inline HYSPLIT generated higher concentrations than the offline approach in the area closest to the release location (200-m and 400-m arcs). The inline

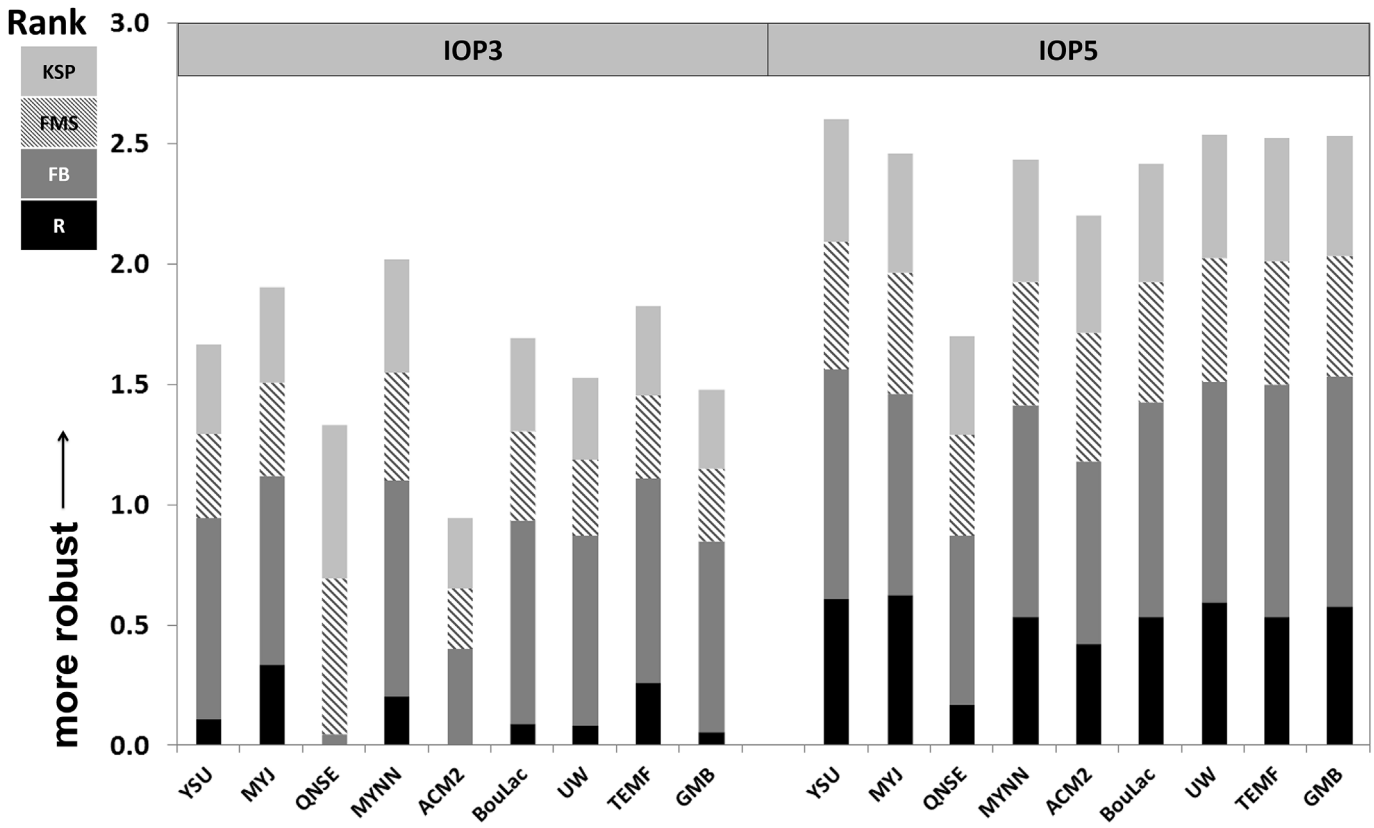

Fig. 7. The statistical Rank of HYSPLIT results using WRF data in 3-km grid spacing corresponding to various PBL schemes for IOP3 and IOP5.

version of HYSPLIT calculates the advection and dispersion processes simultaneously at each integration time step (e.g. 3 s for the domain at 1-km grid spacing). However, the offline HYSPLIT uses a 1-min advection time step and multiple dispersion steps computed within that minute. Hence, the offline approach decouples the advection and dispersion processes, whereas in the inline framework both processes are tightly linked together at each time step. For instance, using the offline approach, a $^{3\ ms\text{-}1}$ wind will advect the tracer 180 m (very close to the first arch at 200 m) in 1 min and then mix it, further illustrating the differences between the two approaches. In particular, for IOP2, the observed plume meandered at different angles over the measurement period while the predicted plume showed a steady pattern toward the northeast missing the observed plume (Fig. 13). The higher concentration near the source generated by the inline approach caused the rank score to be worse than the score of the offline. This finding is consistent with the comparison of the inline and offline simulations performed for the Atmospheric Studies in Complex Terrain (ASCOT) tracer experiment presented by Ngan et al. (2015). The inline calculation tended to keep the plume more intact closer to the release site and therefore maintained higher concentrations at the center of the plume.

Furthermore, we also studied other differences between the inline and offline approaches, besides the advection-dispersion coupling, such as the vertical structure and the meteorological data transfer time frequency. Considering the differences in the vertical structure, the inline system uses WRF's vertical coordinate avoiding vertical interpolation of the meteorological data. The offline HYSPLIT uses its own terrain-following coordinate vertical coordinate (Draxler and Hess 1997) that is generally coarser than the inline setup and thus vertical interpolation is needed. Hence, we altered HYSPLIT's internal layers to get a closer match to the vertical layers used in the inline simulations. The offline results with more layers did not show an improvement over the run with the default vertical layers. The results corresponding to the ASCOT experiment presented by Ngan et al. (2015) showed some improvement when using an increased layer setup over the configuration with less vertical layers. However, ASCOT and the Sagebrush experiment were carried out in different atmospheric conditions. ASCOT was directly influenced by nocturnal drainage flows over a complex terrain, while the Sagebrush experiment was conducted in the afternoon featuring a well-mixed convective boundary layer. We also performed another test to assess the dispersion model sensitivity to the meteorological data frequency. The inline simulation used 3-s data while the offline run used 5-min WRF outputs linearly interpolated to the time step needed for the dispersion calculation. We also conducted an offline HYSPLIT run driven by 1-min WRF data, which is the shortest time step possible for the offline HYSPLIT. However, there was no clear improvement in the rank for the offline result using these 5-and 1-min WRF data.

6. Discussion

The Sagebrush experiment aims to understand the short-range dispersion process from a continuous release near the surface over a flat terrain. The tracer was released on five afternoons in October 2013, under either neutral stability conditions with high wind speeds or unstable conditions with low wind speeds. The measurement array consisted of five arcs 200 m–3200 m away from the release location and samples were taken in 10-min averages. The WRF model was configured with five-nested domains (from 27-km to 0.333-km grid spacing) and different PBL schemes to simulate the meteorological conditions for the tracer release. The model results were evaluated against observations taken during the experiment to understand physical processes relevant to transport and mixing of tracer plumes. We then applied HYSPLIT's inline and offline approaches using the WRF data to model the tracer releases and evaluated the results against concentration measurements. These evaluations shed some light on the capabilities of

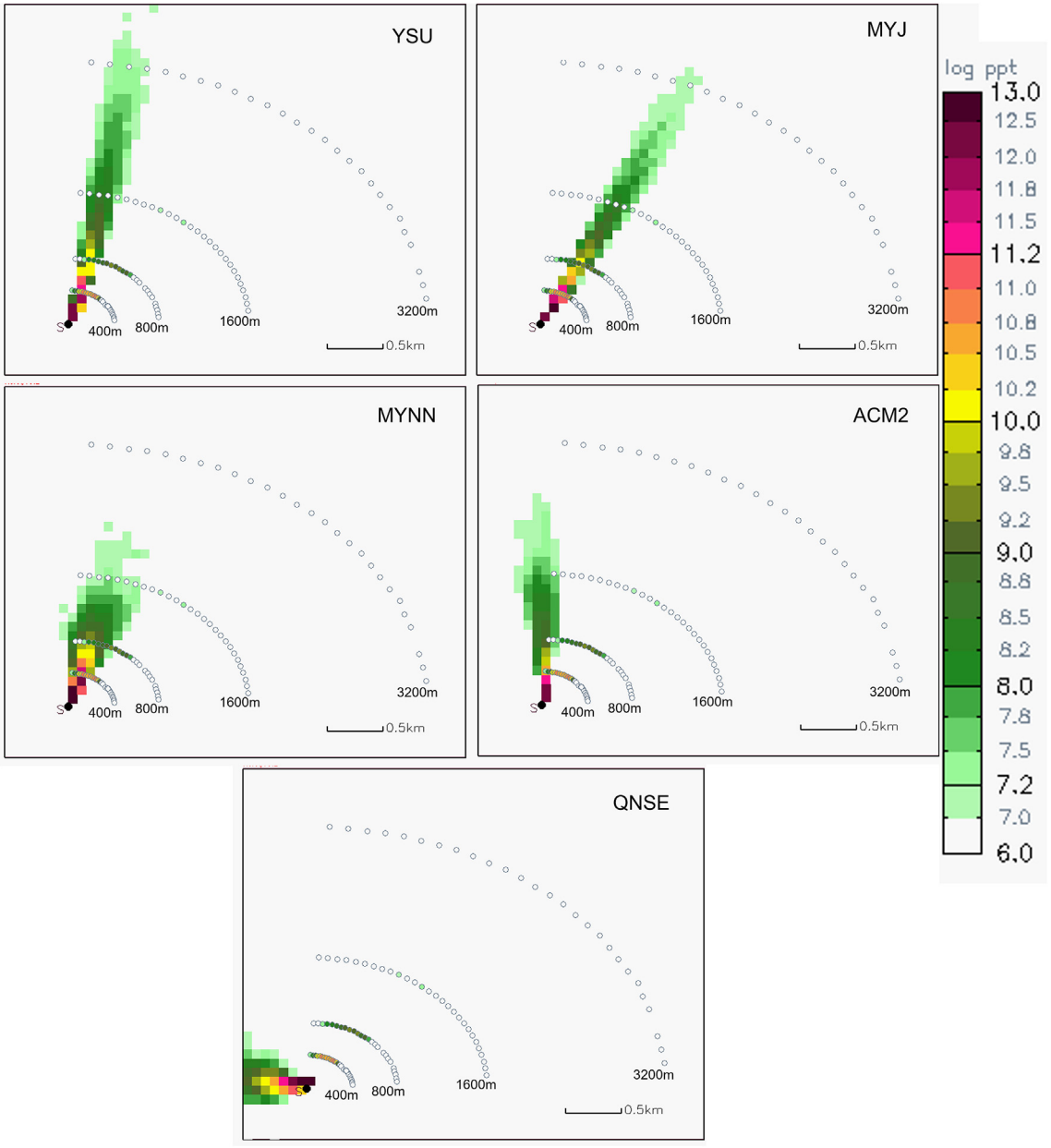

Fig. 8. Tracer concentration plots for IOP 3 at 2000 UTC on October 7th, 2013 from HYSPLIT simulations using 3-km WRF data corresponding to YSU, MYJ, MYNN, ACM2, and QNSE PBL schemes. The shaded color is model concentrations while color-coded circles are measured concentrations. Unit: log ppt. (For interpretation of the references to color in this figure legend, the reader is referred to the Web version of this article.)

both meteorological and dispersion models to simulate fine-scale processes.

Among the five IOPs analyzed, IOP3 featured light winds in the morning rapidly increasing to 8 m/s at about noon. In general, the different meteorological simulations did not capture the strong wind in the afternoon causing a poor simulation of the tracer plume. Large differences were found among the different dispersion simulations driven by the WRF data generated with various PBL schemes. Among them, the MYJ based simulation produced a plume directed in an angle similar to the one measured by the network, while the MYNN plume was wider and pointed more to the north. On the other hand, the YSU plume was narrow and stretched to the outer arc, while the ACM2 plume was off the measurement grid at the beginning of the release. For IOP5, wind flows were southwesterly and relatively stationary generating adequate experimental conditions for the transport of the tracer across the measurement network. In general, the WRF model predicted well the gradual increase in wind and the flow pattern throughout the tracer release. Among all IOP, the dispersion simulation for IOP5 showed the best statistical performance. All the simulations driven by the WRF data using different PBL schemes performed similarly well, except for the case driven by the QNSE meteorology.

The dispersion results show no sensitivity to the horizontal grid resolution of the WRF data used for this kind of well-mixed transport conditions. In addition, we attempted to include subgrid-scale turbulent processes to resolve sub-kilometer features of the experiment by performing WRF runs based on the Shin-Hong PBL scheme and LES. However, the dispersion results driven by these parameterizations were not as good as the runs driven by the data based the other PBL schemes.

The statistical score of the inline simulations was better than that of the offline runs in three out of four releases. The inline HYSPLIT

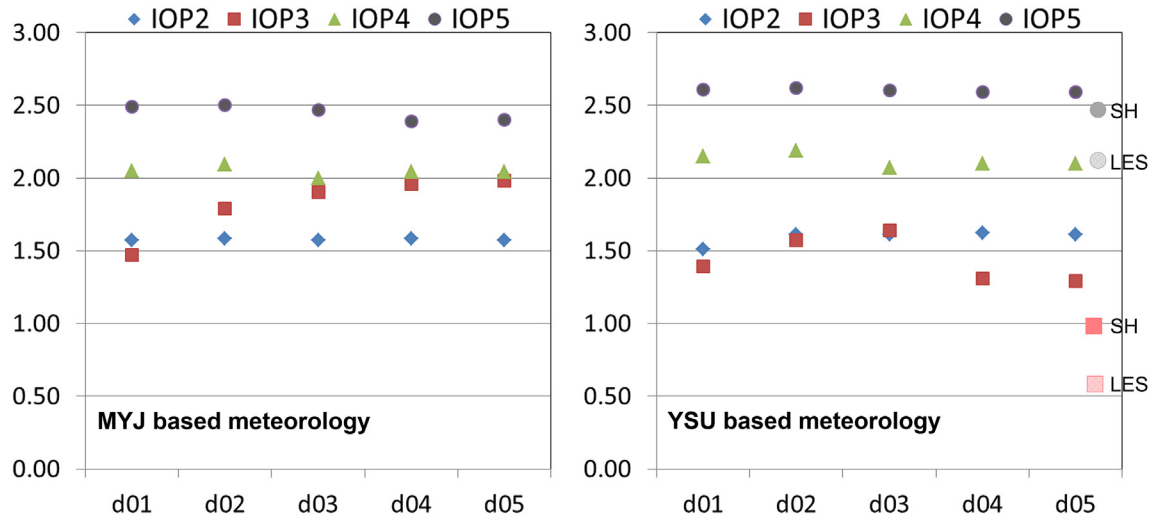

Fig. 9. The statistical rank of HYSPLIT results using MYJ and YSU based meteorology corresponding to the five nested domains in different grid spacing (x-axis). Four additional symbols labeled by "SH" (solid-circle and solid-square) and "LES" (light-circle and light-square) are results driven by WRF data corresponding to Shin-Hong PBL scheme and large-eddy simulation.

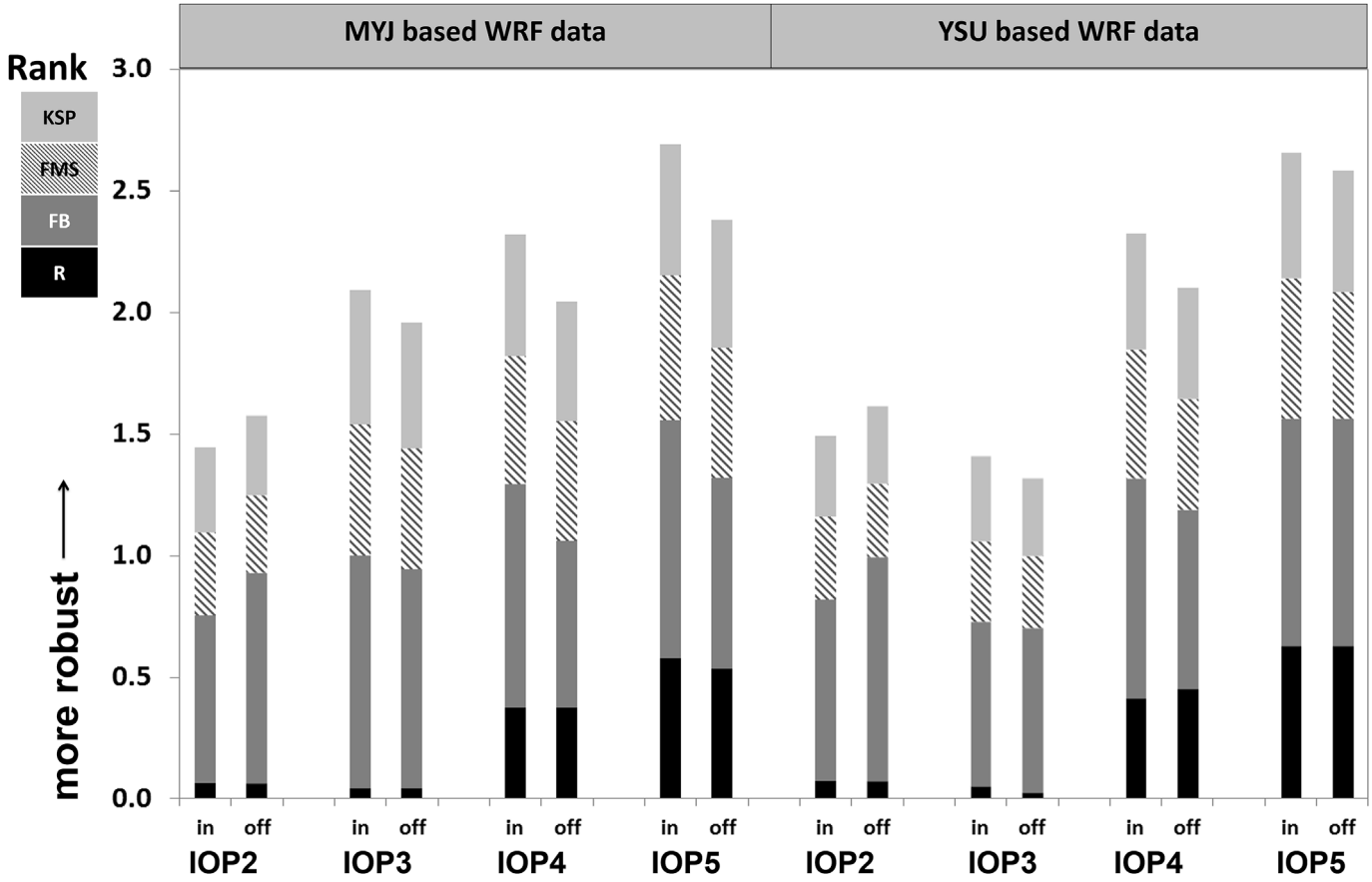

Fig. 10. The statistical Rank of inline and offline HYSPLIT results using MYJ- and YSU-based WRF data in 1-km grid spacing for all IOPs in the Sagebrush experiment.

generated higher concentrations than the offline approach in the area near the release location. The offline approach decouples the advection and dispersion processes (one advection time step with multiple dispersion steps), while in the inline framework both processes are tightly linked together at each time step, given a closer depiction of the physical world.

This study advances the understanding of the performance of the WRF-HYSPLIT modeling system for dispersion scenarios influenced by the different daytime stability conditions at fine spatial (a few hundred meters) and temporal (10-min averaging) scales. HYSPLIT simulated the trace plumes well as the WRF model provided accurate meteorological data for the plume calculation for weakly unstable conditions

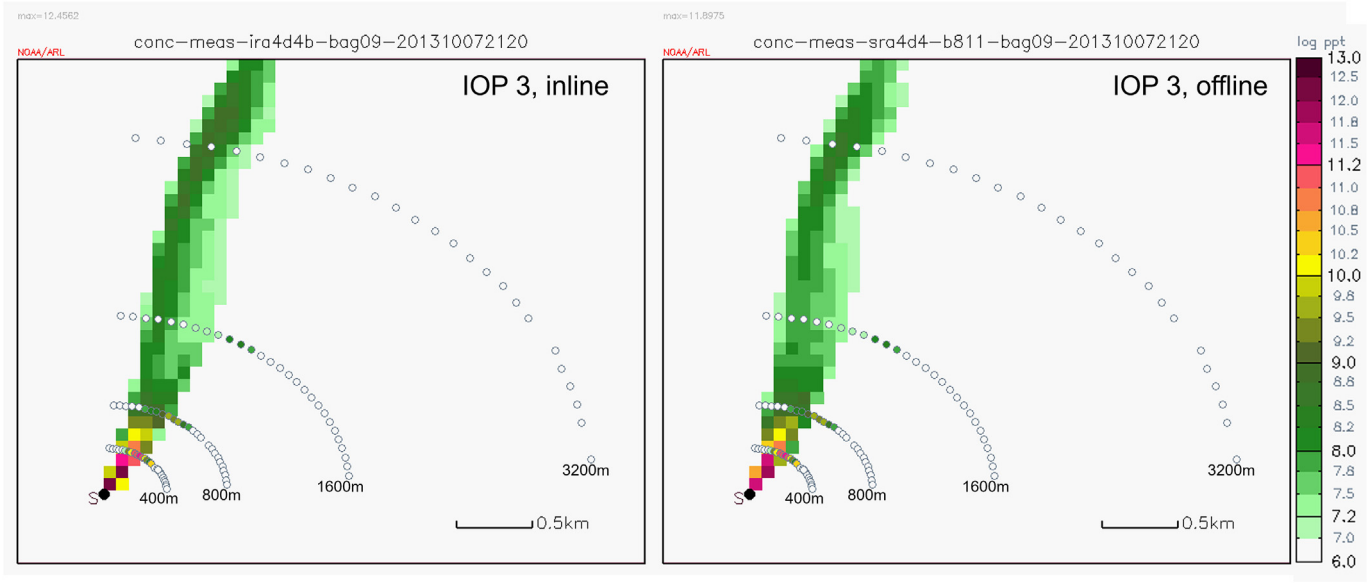

Fig. 11. Tracer concentration plots for IOP 3 at 2120 UTC on October 7th, 2013 from inline (left) and offline (right) HYSPLIT simulations using 1-km WRF data. The shaded color is model concentrations while color-coded circles are measured concentrations. Unit: log ppt. (For interpretation of the references to color in this figure legend, the reader is referred to the Web version of this article.)

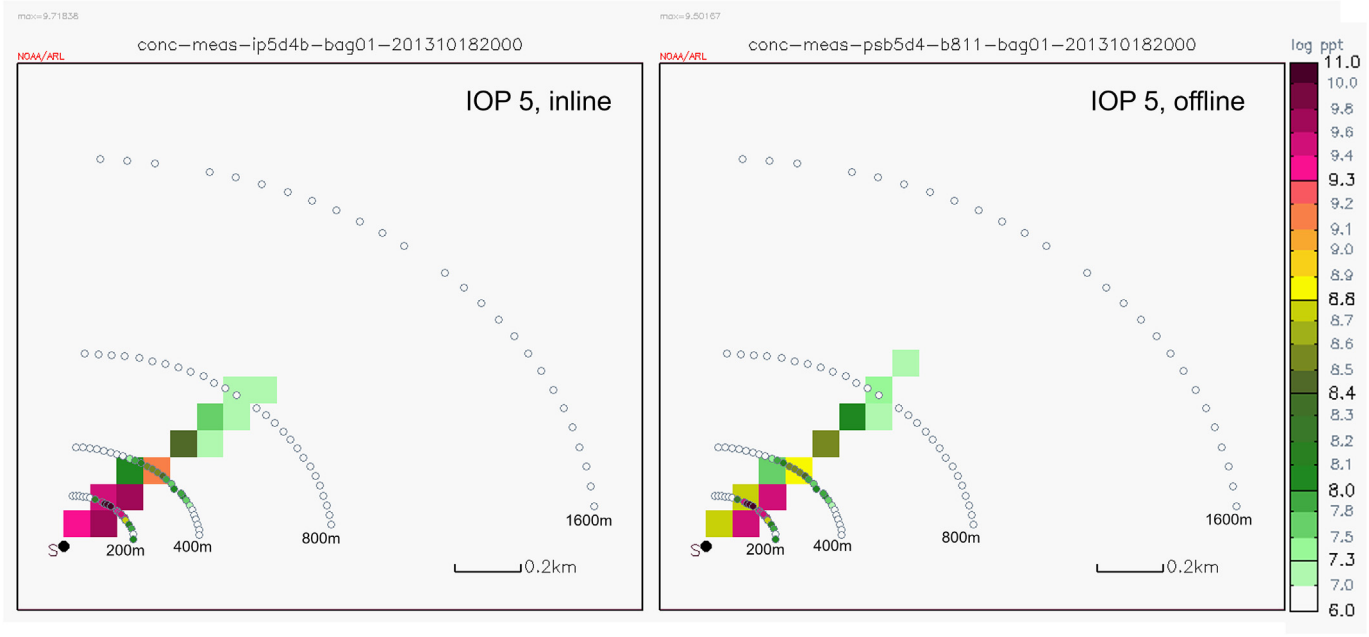

Fig. 12. Tracer concentration plots for IOP 5 at 2000 UTC on October 18th, 2013 from inline (left) and offline (right) HYSPLIT simulations using 1-km WRF data. The shaded color is model concentrations while color-coded circles are measured concentrations. Unit: log ppt. (For interpretation of the references to color in this figure legend, the reader is referred to the Web version of this article.)

featuring moderate southwesterly winds (IOP4 and IOP5). However, HYSPLIT's performance was degraded under neutral conditions with strong winds (IOP3) and unstable conditions with light winds (IOP2) due to the underestimation of the strong winds or the inaccurate prediction of wind direction. Independent of the impact of the uncertainty of the meteorological data on the dispersion results, the inline coupled simulations consistently show higher concentrations in the area a few hundred meters downwind of the release location when compared with the offline results. This is explained by the tight linkage between the dispersion and the advection processes in the inline model framework. Future works will include the investigation of different approaches to estimate turbulent velocity variances in HYSPLIT based available measurement from the Sagebrush tracer experiment to further understand vertical mixing process.

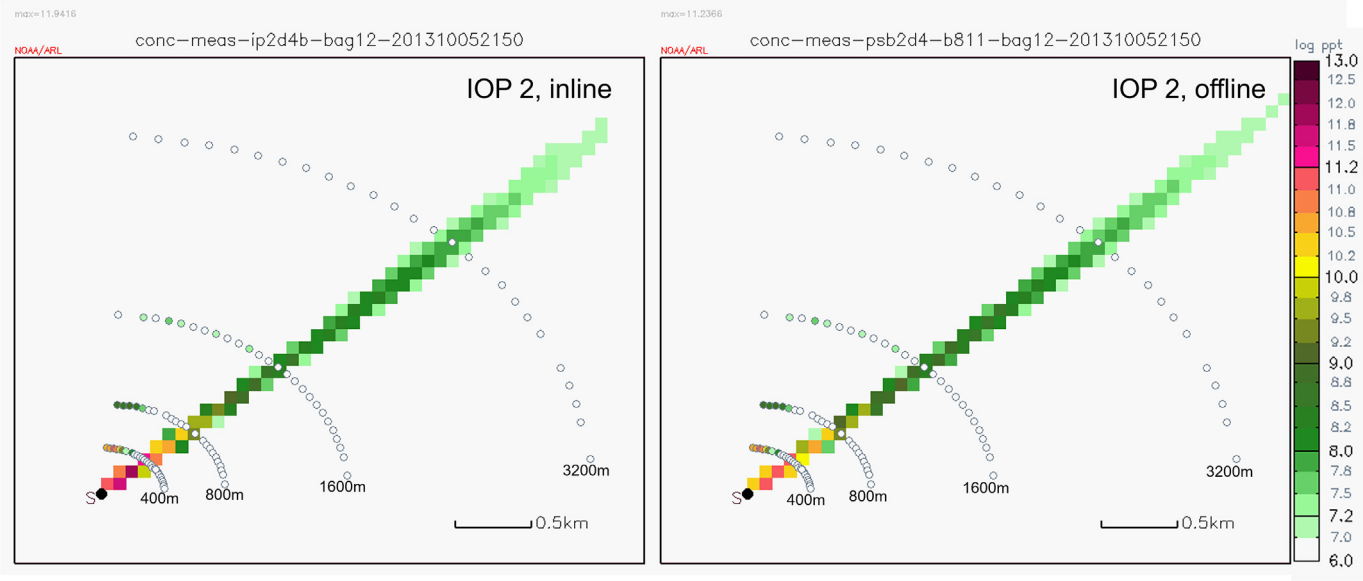

Fig. 13. Tracer concentration plots for IOP 2 at 2150 UTC on October 10th, 2013 from inline (left) and offline (right) HYSPLIT simulations using 1-km WRF data. The shaded color is model concentrations while color-coded circles are measured concentrations. Unit: log ppt. (For interpretation of the references to color in this figure legend, the reader is referred to the Web version of this article.)

Acknowledgments

The authors thank these people for their contribution to the Sagebrush Tracer Experiment: K.L. Clawson, R.G. Carter, J.D. Rich, T.W. Strong, S.A. Beard, B.R. Reese, and D. Davis from NOAA/ARL's Field Research Division; H. Liu, E. Russell, Z. Gao from Washington State University (participation was partly supported by the National Science Foundation Division of Atmospheric and Geospace Sciences under Grant 1112938); and S. Brooks from University of Tennessee Space Institute.

References

Angevine, W.M., Jiang, H.L., Mauritsen, T., 2010. Performance of an eddy diffusivity–mass flux scheme for shallow cumulus boundary layers. Mon. Weather Rev. 138, 2895–2912.

Barlow, J., Best, M., Bohnenstengel, S.I., Clark, P., Grimmond, S., Lean, H., Christen, A., Emeis, S., Haeffelin, M., Harman, I.N., Lemonsu, A., Martilli, A., Pardyjak, E., Rotach, M.W., Ballard, S., Boutle, I., Brown, A., Cai, X., Carpentieri, M., Coceal, O., Crawford, B., Di Sabatino, S., Dou, J., Drew, D.R., Edwards, J.M., Fallmann, J., Fortuniak, K., Gornall, J., Gronemeier, T., Halios, C.H., Hertwig, D., Hirano, K., Holtslag, A.A.M., Luo, Z., Mills, G., Nakayoshi, M., Pain, K., Schlunzen, K.H., Smith, S., Soulhac, L., Steeneveld, G., Sun, T., Theeuwes, N.E., Thomson, D., Voogt, J.A., Ward, H.C., Xie, Z., Zhong, J., 2017. Developing a research strategy to better understand, observe, and simulate urban atmospheric processes at kilometer to subkilometer scales. Bull. Am. Meteorol. Soc. 98, 10 ES261-ES264.

Bougeault, P., Lacarrere, P., 1989. Parameterization of orography-induced turbulence in a mesobeta-scale model. Mon. Weather Rev. 117, 1872–1890.

Bretherton, C.S., Park, S., 2009. A new moist turbulence parameterization in the community atmosphere model. J. Clim. 22, 3422–3448.

Chai, T., Draxler, R., Stein, A., 2015. Source term estimation using air concentration measurements and a Lagrangian dispersion model – experiments with pseudo and real cesium-137 observations from the Fukushima nuclear accident. Atmos. Environ. 106, 241–251.

Chai, T., Crawford, A., Stunder, B., Pavolonis, M.J., Draxler, R., Stein, A., 2017. Improving volcanic ash predictions with the HYSPLIT dispersion model by assimilating MODIS satellite retrievals. Atmos. Chem. Phys. 17, 2865–2879.

Chen, F., Dudhia, J., 2001. Coupling and advanced land surface–hydrology model with the Penn State–NCAR MM5 modeling system. Part I: model implementation and sensitivity. Mon. Weather Rev. 129, 569–585.

Cohen, M., Draxler, R., Artz, R., 2013. Modeling atmospheric mercury deposition to the Great Lakes: Examination of the influence of variations in model inputs, parameters, and algorithms on model results. NOAA Air Resources Laboratory Final Rep. for work conducted with FY2011 funding from the Great Lakes Restoration Initiative, 157 pp. Available online at. www.arl.noaa.gov/documents/reports/GLRI_FY2011_Atmospheric_Mercury_Final_Report_2013_June_30.pdf.

Crawford, A.M., Stunder, B.J.B., Ngan, F., Pavolonis, M.J., 2016. Initializing HYSPLIT with satellite observations of volcanic ash: a case study of the 2008 Kasatochi eruption. J. Geophys. Res.: Atmosphere 121, 10786–10803.

Deng, A., Stauffer, D., Gaudet, B., Dudhia, J., Hacker, J., Bruyere, C., Wu, W., Vandenberghe, F., Liu, Y., Bourgeois, A., 2009. Update OnWRF-ARWend-to-end Multi-scale FDDA System. 10th WRF Users Workshop. NCAR, Boulder, CO 1.9.

Draxler, R.R., Hess, G.D., 1997. Description of the HYSPLIT_4 Modeling System. NOAA Tech. Memo. ERL ARL-224. NOAA/Air Resources Laboratory, Silver Spring, MD 24 pp. [Available online at: http://www.arl.noaa.gov/documents/reports/arl-224.pdf.

Draxler, R.R., 2006. The use of global and mesoscale meteorological model data to predict the transport and dispersion of tracer plumes over Washington, D.C. Wea. Forecasting 21, 383–394.

Dudhia, J., Wang, W., 2014. WRF Advanced Usage and Best Practices. 15th WRF Users Workshop. National Center for Atmospheric Research, Boulder, CO 35 pp. [Available online at: http://www2.mmm.ucar.edu/wrf/users/workshops/WS2014/ppts/best_prac_wrf.pdf.

Eslinger, P.W., Bowyer, T.W., Achim, P., Chai, T., Deconninck, B., Freeman, K., Generoso, S., Hayes, P., Heidmann, V., Hoffman, I., Kijima, Y., Krysta, M., Malo, A., Maurer, C., Ngan, F., Robins, P., Ross, J.O., Saunier, O., Schlosser, C., Schoppner, M., Schrom, B.T., Seibert, P., Stein, A.F., Ungar, K., Yi, J., 2016. International challenge to predict the impact of radioxenon releases from medical isotope production on a comprehensive nuclear test ban treaty sampling station. J. Environ. Radioact. 157, 41–51.

Finn, D., Clawson, K.L., Eckman, R.M., Carter, R.G., Rich, J.D., Strong, T.W., Beard, S.A., Reese, B.R., Davis, D., Liu, H., Russell, E., Gao, Z., Brooks, S., 2015. Project Sagebrush Phase 1. NOAA Tech Memo OAR ARL-268. 362 pp.

Finn, D., Clawson, K.L., Eckman, R.M., Liu, H., Russell, E.S., Gao, Z., Brooks, S., 2016. Project Sagebrush: revisiting the value of the horizontal plume spread parameter σy. J. Appl. Meteor. Climatol. 55, 1305–1322. http://dx.doi.org/10.1175/JAMC-D-15-0283.1.

Gibbs, J.A., Fedorovich, E., Van Eijk, A.M.J., 2011. Evaluating Weather Research and Forecasting (WRF) model predictions of turbulent flow parameters in a dry convective boundary layer. J. Appl. Meteor. Climatol. 50, 2429–2444.

Grell, G.A., Freitas, S., 2013. A scale and aerosol aware stochastic convective parameterization for weather and air quality modeling. Atmos. Chem. Phys. Discuss. 13, 23845–23893. http://dx.doi.org/10.5194/acpd-13-23845-2013.

Grell, G.A., Dudhia, J., Stauffer, D., 1994. A Description of the Fifth Generation Penn State/NCAR Mesoscale Model (MM5). NCAR Tech. Note NCAR/TN-3981STR. 121 pp.

Grenier, H., Bretherton, C.S., 2001. A moist PBL parameterization for large-scale models and its application to subtropical cloud-topped marine boundary layers. Mon. Weather Rev. 129, 357–377.

Hegarty, J., Draxler, R.R., Stein, A.F., Brioude, J., Mountain, M., Eluszkiewicz, J., Nehrkorn, T., Ngan, F., Andrews, A., 2013. Validation of Lagrangian particle dispersion models with measurements from controlled tracer releases. J. Appl. Meteor. Climatol. 52, 2623–2637.

Hong, S.-Y., Dudhia, J., Chen, S.-H., 2004. A revised approach to ice microphysical processes for the bulk parameterization of clouds and precipitation. Mon. Weather Rev. 132, 103–120.

Hong, S.Y., Noh, Y., Dudhia, J., 2006. A new vertical diffusion package with an explicit treatment of entrainment processes. Mon. Weather Rev. 134, 2318–2341.

Iacono, M.J., Delamere, J.S., Mlawer, E.J., Shephard, M.W., Clough, S.A., Collins, W.D., 2008. Radiative forcing by long-lived greenhouse gases: calculations with the AER radiative transfer models. J. Geophys. Res. 113, D13103,. http://dx.doi.org/10.1029/2008JD009944.

Janjic, Z.I., 1994. The step-mountain eta coordinate model: further developments of the convection, viscous sublayer, and turbulence closure schemes. Mon. Weather Rev. 122, 927–945.
Leadbetter, S.J., Hort, M.C., Jones, A.R., Webster, H.N., Draxler, R.R., 2015. Sensitivity of the modelled deposition of caesium-137 from the Fukushima Dai-Ichi nuclear power plant to the wet deposition parameterisation in NAME. J. Environ. Radioact. 139, 200–211.
Mesinger, F., Dimego, G., Kalnay, E., Mitchell, K., Shafran, P.C., Ebisuzaki, W., Jovic, D., Woollen, J., Rogers, E., Berbery, E.H., Ek, M.B., Fan, Y., Grumbine, R., Higgins, W., Li, H., Lin, Y., Manikin, G., Parrish, D., Shi, W., 2006. North American regional Reanalysis. Bull. Am. Meteorol. Soc. 87, 343–360.
Nakanishi, M., Niino, H., 2006. An improved mellor–yamada Level-3 model: its numerical stability and application to a regional prediction of advection fog. Bound.-Layer Meteor. 119, 397–407.
Ngan, F., Cohen, M., Luke, W., Ren, X., Draxler, R.R., 2015. Meteorological modeling using WRF-ARW model for grand bay intensive studies of atmospheric mercury. Atmosphere 6, 209–233.
Pergaud, J., Masson, V., Malardel, S., Couvreux, F., 2009. A parameterization of dry thermals and shallow cumuli for mesoscale numerical weather prediction. Bound.-Layer Meteor. 132, 83–106.
Pliem, J.E., 2007. A combined local and nonlocal closure model for the atmospheric boundary layer. Part I: model description and testing. J. Appl. Meteor. Climatol. 46, 1383–1395.
Powers, J.G., Klemp, J.B., Skamarock, W.C., Davis, C.A., Dudhia, J., Gill, D.O., Coen, J.L., Gochis, D.J., Ahmadov, R., Peckham, S.E., Grell, G.A., Michalakes, J., Trahan, S., Benjamin, S.G., Alexander, C.R., Dimego, G.J., Wang, W., Schwartz, C.S., Romine, G.S., Liu, Z., Snyder, C., Chen, F., Barlage, M.J., Yu, w., Duda, M.G., 2017. The weather research and forecasting model: overview, system efforts, and future directions. Bull. Am. Meteorol. Soc. 98 (8), 1717–1737.
Rolph, G., Stein, A., Stunder, B., 2017. Real-time environmental applications and display sYstem: READY. Environ. Model. Software 95, 210–228.
Shin, H.H., Dudhia, J., 2016. Evaluation of PBL parameterizations in WRF at subkilometer grid spacings: turbulence statistics in the dry convective boundary layer. Mon. Weather Rev. 144, 1161–1177.
Shin, H.H., Hong, S.Y., 2015. Representation of the subgrid-scale turbulent transport in convective boundary layers at gray-zone resolutuions. Mon. Weather Rev. 143, 250–271.
Simsek, V., Pozzoli, L., Unal, A., Kindap, T., Karaca, M., 2014. Simulation of Cs-137 transport and deposition after the chernobyl nuclear power plant accident and radiological doses over the anatolian peninsula. Sci. Total Environ. 499, 74–88.
Skamarock, W.C., Klemp, J.B., Dudhia, J., Gill, D.O., Barker, D.M., Duda, M.G., Huang, X., Wang, W., Powers, J.G., 2008. A Description of the Advanced Research WRF Verson 3. NCAR Tech Note NCAR/TN-4751STR. 125 pp.
Stein, A.F., Draxler, R.R., Rolph, G.D., Stunder, B.J.B., Cohen, M.D., Ngan, F., 2015. NOAA's HYSPLIT atmospheric transport and dispersion modeling system. Bull. Am. Meteorol. Soc. 96, 2059–2077.
Stien, A.F., Isakov, V., Godowitch, J., Draxler, R.R., 2007. A hybrid modeling approach to resolve pollutant concentrations in an urban area. Atmos. Environ. 41, 9410–9426. http://dx.doi.org/10.1016/j.atmosenv.2007.09.004.
Sun, X., Holmes, H.A., Osibanjo, O.O., Sun, Y., Ivey, C.E., 2017. Evaluation of surface fluxes in the WRF model: case study for farmland in rolling terrain. Atmosphere 8 (10), 197. http://dx.doi.org/10.3390/atmos8100197.
Wyngaard, J.C., 2004. Toward numerical modeling in the “terra incognita.”. J. Atmos. Sci. 61, 1816–1826.
Xiu, A., Pleim, J.E., 2001. Development of a land surface model. Part I: application in a mesoscale meteorological model. J. Appl. Meteorol. 40, 192–209.